

[Me₄N](Ni^{II}(BEAAM)): A Synthetic Model for Nickel Superoxide Dismutase That Contains Ni in a Mixed Amine/Amide Coordination Environment

Jason Shearer* and Ningfeng Zhao

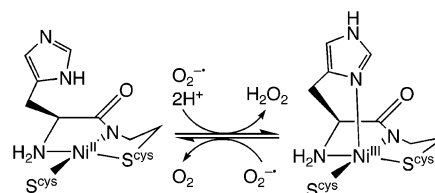
Department of Chemistry/216, University of Nevada, Reno, Reno, Nevada 89557

Received August 24, 2006

Nickel superoxide dismutase (NiSOD) is a metalloenzyme that converts O₂^{•−} into H₂O₂ and O₂ by cycling between Ni^{II} and Ni^{III} oxidation states. Reduced NiSOD contains Ni^{II} in a square-planar N₂S₂ coordination environment formed by two cysteinyl S atoms, an amide N, and an amine N to Ni^{II}. [Me₄N](Ni^{II}(BEAAM)) represents the first NiN₂S₂ complex containing Ni in a mixed amine/amide environment. [Me₄N](Ni^{II}(BEAAM)) contains Ni–S bonds at 2.177(2) and 2.137(2) Å and Ni–N bonds at 1.989(7) and 1.858(6) Å, which compare well with the metalloenzyme. Orange solutions of [Me₄N](Ni^{II}(BEAAM)) in MeCN are diamagnetic and stable toward O₂ for weeks. A quasireversible Ni^{II/III} redox couple is observed for [Ni^{II}(BEAAM)](NMe₄) at 0.12(1) V vs Ag/AgCl. These data suggest that NiSOD utilizes the mixed amine/amide ligands to modulate the Ni^{II/III} redox couple to best match the O₂^{•−} reduction/oxidation couples while maintaining O₂ stability.

Superoxide (O₂^{•−}) is a cellular toxin that is typically degraded by superoxide dismutases (SODs), which catalyze the disproportionation of O₂^{•−} into O₂ and H₂O₂.^{1,2} The most recently discovered SOD contains Ni in its active site (NiSOD) and catalyzes the disproportionation of O₂^{•−} by cycling between the Ni^{II} and Ni^{III} oxidation states (Scheme 1).³ In the reduced state, the Ni center is contained within a square-planar N₂S₂ ligand environment with ligands derived from two cysteinyl residues, one amide N from the peptide backbone and one amine N from the free N-terminal amine.^{4,5} Upon oxidation to Ni^{III}, an axial imidazole N coordinates to Ni. Despite the fact that the structure of NiSOD is known,

Scheme 1



many questions remain concerning the mechanism of SOD catalysis and how the NiSOD primary coordination sphere contributes to reactivity. One question concerns why NiSOD utilizes an anionic amide and the free amine N as ligands to Ni, which are both unusual biological ligands.

NiN₂S₂ complexes can be reactive toward both H₂O₂ and O₂, often yielding S-based oxygenation.⁶ Synthetic studies have demonstrated that NiN₂S₂ complexes in bis-amine ligand environments are more stable toward O₂ than the corresponding bis-amide complexes.^{7,8} This might suggest that NiSOD utilizes the amine/amide coordination motif to protect itself from S oxygenation. To determine exactly how the N^{amine}N^{amide}S₂ coordination motif influences the electronics, redox properties, and stability of NiN₂S₂ complexes, we prepared [Me₄N](Ni^{II}(BEAAM)),⁹ which is the first small-molecule NiN₂S₂ complex with amine and amide ligands to Ni.

The ligand BEAAM was prepared according to the procedure outlined in Figure 1 (see the Supporting Information). BEAAM was then metalated under anaerobic conditions using NiCl₂ in methanol. Cation exchange with [Me₄N]Cl yielded [Me₄N](Ni^{II}(BEAAM)). Subsequent crystallization from MeCN/Et₂O produced the purified product. The X-ray crystal structure of [Me₄N](Ni^{II}(BEAAM))·MeCN·H₂O shows that Ni^{II} is contained within a square plane with ligands derived from the amine and amide N

* To whom correspondence should be addressed. E-mail: shearer@chem.unr.edu.

- (1) Miller, A.-F. *Curr. Opin. Chem. Biol.* **2004**, *8*, 162–168.
- (2) Valentine, J. S.; Wertz, D. L.; Lyons, T. J.; Liou, L.-L.; Goto, J. J.; Gralla, E. B. *Curr. Opin. Chem. Biol.* **1998**, *2*, 253–262.
- (3) (a) Youn, H.-D.; Kim, E.-J.; Roe, J.-H.; Hah, Y. C.; Kang, S.-O. *Biochem. J.* **1996**, *318*, 889–896. (b) Youn, H.-D.; Youn, H.; Lee, J.-W.; Yim, Y.-I.; Lee, J. K.; Hah, Y. C.; Kang, S.-O. *Arch. Biochem. Biophys.* **1996**, *334*, 341–348.
- (4) Barondeau, D. P.; Kassmann, C. J.; Bruns, C. K.; Tainer, J. A.; Getzoff, E. D. *Biochemistry* **2004**, *43*, 8038–8047.
- (5) Wuerges, J.; Lee, J.-W.; Yim, Y.-I.; Yim, H.-S.; Kang, S.-O.; Carugo, K. D. *Proc. Natl. Acad. Sci. U.S.A.* **2004**, *101*, 8569–8574.

- (6) Grapperhaus, C. A.; Darenbourg, M. Y. *Acc. Chem. Res.* **1998**, *31*, 451–459.
- (7) Grapperhaus, C. A.; Mullins, C. S.; Kozlowski, P. M.; Mashuta, M. S. *Inorg. Chem.* **2004**, *43*, 2859–2866.
- (8) Hatlevik, O.; Blanksma, M. C.; Mathrubootham, V.; Arif, A. M.; Hegg, E. L. *J. Biol. Inorg. Chem.* **2004**, *9*, 238–246.
- (9) BEAAM: *N*-{2-[benzyl(2-mercapto-2-methylpropyl)amino]ethyl}-2-mercapto-2-methylpropanamide.

COMMUNICATION

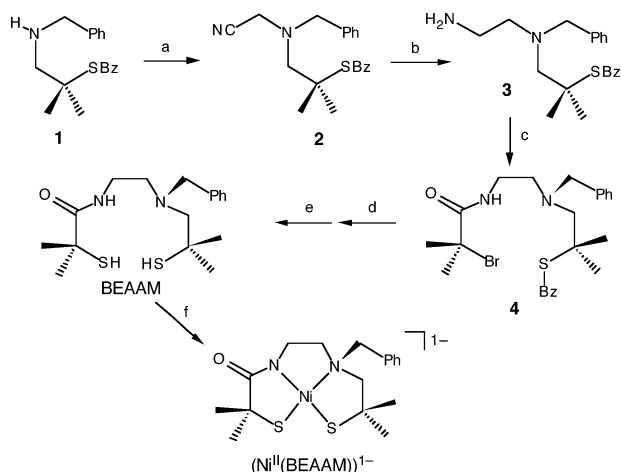


Figure 1. Synthesis of $(\text{Ni}^{\text{II}}(\text{BEAAM}))^-$: (a) BrCH_2CN , K_2CO_3 , NaI , MeCN , 8 h (reflux); (b) AlH_3 , THF , 12 h (reflux); (c) 2-bromo-2-methylpropionyl bromide, Et_3N , CH_2Cl_2 , 12 h (room temperature); (d) benzylmercaptan, KOH , EtOH , 12 h (reflux); (e) Na , $\text{NH}_3(\text{l})$, 1 h (-78°C); (f) NiCl_2 , Me_4NCl , NaOMe , MeOH , 12 h (room temperature).

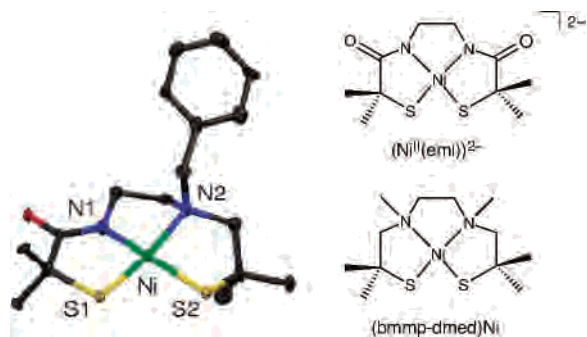


Figure 2. Left: thermal ellipsoid plot (50% probability) displaying the anion from $[\text{Me}_4\text{N}][\text{Ni}^{\text{II}}(\text{BEAAM})] \cdot \text{MeCN} \cdot \text{H}_2\text{O}$. Selected bond lengths (\AA) and angles (deg): $\text{Ni}-\text{N}1$, 1.858(6); $\text{Ni}-\text{N}2$, 1.989(7); $\text{Ni}-\text{S}1$, 2.137(2); $\text{Ni}-\text{S}2$, 2.177(2); $\text{N}1-\text{Ni}-\text{S}1$, 88.3(2); $\text{S}1-\text{Ni}-\text{S}2$, 97.52(8); $\text{S}2-\text{Ni}-\text{N}2$, 90.0(2); $\text{N}2-\text{Ni}-\text{N}1$, 85.8(3). Right: representations of $(\text{Ni}^{\text{II}}(\text{emi}))^{2-}$ and $(\text{bmmp-dmed})\text{Ni}$.

atoms and the two thiolate S atoms (Figure 2).¹⁰ As expected, the $\text{Ni}-\text{N}^{\text{amide}}$ distance [$\text{N}1$; 1.858(6) \AA] is shorter than the $\text{Ni}-\text{N}^{\text{amine}}$ distance [$\text{N}2$; 1.989(7) \AA]. There is also asymmetry in the $\text{Ni}-\text{S}$ distances, with the $\text{Ni}-\text{S}$ bond trans to the amine ($\text{S}1$) being shorter than the one trans to the amide ($\text{S}2$) [2.177(2) vs 2.137(2) \AA]. This should be expected considering that N^{amide} ligands are stronger σ donors than N^{amine} ligands and therefore should display a larger trans influence. These metrical parameters compare well with Ni -ligand distances from bis-amide and bis-amine NiN_2S_2 complexes^{6-8,11-14} and reduced NiSOD .^{4,5,14} The crystal

structure for reduced NiSOD displays a $\text{Ni}-\text{N}^{\text{amine}}$ bond length of 1.87(6) \AA and a $\text{Ni}-\text{N}^{\text{amide}}$ bond length of 1.91(3) \AA , while EXAFS data place the average $\text{Ni}-\text{N}$ bond length at 1.91(1) \AA . The $\text{Ni}-\text{S}$ bond lengths derived from the NiSOD crystal structure are 2.16(2) \AA (trans to the amine) and 2.19(2) \AA (trans to the amide), while EXAFS places the average $\text{Ni}-\text{S}$ bond length in the enzyme at 2.160(4) \AA . These minor differences in the Ni -ligand bond lengths of NiSOD vs $(\text{Ni}^{\text{II}}(\text{BEAAM}))^-$ could be the result of strain induced by the chelate ring size of $(\text{Ni}^{\text{II}}(\text{BEAAM}))^-$, which may not be present in NiSOD .^{11b}

Density functional theory (DFT) studies were used to probe the differences in the bonding and energetics of $(\text{Ni}^{\text{II}}(\text{BEAAM}))^-$ vs the structurally related bis-amine and bis-amide complexes $(\text{bmmp-dmed})\text{Ni}^7$ and $(\text{Ni}^{\text{II}}(\text{emi}))^{2-}$ ¹¹ (Figure 2 and the Supporting Information). These calculations suggest that for the three NiN_2S_2 complexes the degree of S character in the $\text{Ni}/\text{S}(\pi)^*$ highest occupied molecular orbital (HOMO) decreases as the number of amides to Ni increases (52.1% vs 31.8% vs 21.0%), as was previously demonstrated for other systems.¹⁵⁻¹⁷ Furthermore, when the orbital energies are normalized to the HOMO, the $\text{Ni}(3d_{x^2-y^2})/\text{S}/\text{N}(\sigma)^*$ orbital progressively increases in energy relative to the HOMO as more anionic amide donors are added to the primary coordination sphere. This is in line with the increase in σ donation along the xy plane as the neutral amine donors are replaced with anionic amides. Grapperhaus and co-workers have found similar systematic changes in a recent DFT study exploring the influence of amide coordination on NiN_2S_2 complexes.¹⁷

Diamagnetic orange solutions of $[\text{Me}_4\text{N}][\text{Ni}^{\text{II}}(\text{BEAAM})]$ yield electronic absorption spectra with a low-energy shoulder at 17 980 cm^{-1} ($\epsilon = 70 \text{ M}^{-1} \text{ cm}^{-1}$) and defined peaks at 21 690 cm^{-1} ($\epsilon = 290 \text{ M}^{-1} \text{ cm}^{-1}$) and 37 450 cm^{-1} ($\epsilon = 21 500 \text{ M}^{-1} \text{ cm}^{-1}$; Figure 3). The two low-energy features, which correspond to ligand-field transitions, compare well with both reduced NiSOD ¹⁶ and $[\text{Ni}^{\text{II}}(\text{SOD}^{\text{M}})]$ (a metalloprotein-based NiSOD mimic that displays SOD activity).¹⁸ Reduced NiSOD displays a peak at 22 240 cm^{-1} and a shoulder at 17 770 cm^{-1} , while $[\text{Ni}^{\text{II}}(\text{SOD}^{\text{M}})]$ displays these features at 21 800 and 18 100 cm^{-1} . Therefore, the electronic character of $[\text{Me}_4\text{N}][\text{Ni}^{\text{II}}(\text{BEAAM})]$ is similar to the two known compounds that contain Ni^{II} in an $\text{N}^{\text{amine}}\text{N}^{\text{amide}}\text{S}_2$ coordination environment. These features are also consistent with the structurally related NiN_2S_2 complexes $[\text{Et}_4\text{N}]_2(\text{Ni}^{\text{II}}(\text{emi}))$ and $(\text{bmmp-dmed})\text{Ni}$.^{7,11} Bis-amide-ligated $[\text{Et}_4\text{N}]_2(\text{Ni}^{\text{II}}(\text{emi}))$ displays peaks in the visible region at 23 040 cm^{-1} ($\epsilon = 340 \text{ M}^{-1} \text{ cm}^{-1}$) and 18 180 nm ($\epsilon = 79 \text{ M}^{-1} \text{ cm}^{-1}$), while bis-amine-ligated $(\text{bmmp-dmed})\text{Ni}$ displays a peak at 20 990 cm^{-1} ($\epsilon = 260 \text{ M}^{-1} \text{ cm}^{-1}$) and a shoulder at 15 720 cm^{-1} ($\epsilon = 60 \text{ M}^{-1} \text{ cm}^{-1}$; Figure 3). The systematic shifts of

(10) Crystallographic data were collected on a Bruker APEX CCD diffractometer (Mo $\text{K}\alpha$ radiation). $[\text{Me}_4\text{N}][\text{Ni}^{\text{II}}(\text{BEAAM})] \cdot \text{MeCN} \cdot \text{H}_2\text{O}$: $\text{C}_{23}\text{H}_{40}\text{N}_4\text{NiS}_2\text{O}_2$, MW = 527.42, $T = 100(1) \text{ K}$, monoclinic, $C2/c$, $Z = 8$, $a = 38.9762(14) \text{ \AA}$, $b = 7.4408(3) \text{ \AA}$, $c = 18.9276(6) \text{ \AA}$, $\beta = 104.423(2)^\circ$, $V = 5316.3(3) \text{ \AA}^3$, 21 460 measured reflections, 3458 independent reflections, $R1 = 0.0779$, and $wR2 = 0.1795$.
 (11) (a) Krüger, H.-J.; Peng, G.; Holm, R. H. *Inorg. Chem.* **1991**, *30*, 734-742. (b) Rao, P. V.; Bhaduri, S.; Jiang, J.; Holm, R. H. *Inorg. Chem.* **2004**, *43*, 5833-5849.
 (12) (a) Farmer, P. J.; Reibenspies, J. H.; Lindahl, P. A.; Darensbourg, M. Y. *J. Am. Chem. Soc.* **1993**, *115*, 4665-4674. (b) Musie, G.; Reibenspies, J. H.; Darensbourg, M. Y. *Inorg. Chem.* **1998**, *37*, 302-310.
 (13) Krishnan, R.; Voo, J. K.; Riordan, C. G.; Zahkarov, L.; Rheingold, A. L. *J. Am. Chem. Soc.* **2003**, *125*, 4422-4423.

(14) Choudhury, S. B.; Lee, J.-W.; Davidson, G.; Yim, Y.-I.; Bose, K.; Sharma, M. L.; Kang, S.-O.; Cabelli, D. E.; Maroney, M. J. *Biochemistry* **1999**, *38*, 3744-3752.
 (15) Neupane, K. P.; Shearer, J. *Inorg. Chem.* **2006**, in press.
 (16) Fiedler, A. T.; Bryngelson, P. A.; Maroney, M. J.; Brunold, T. C. *J. Am. Chem. Soc.* **2005**, *127*, 5449-5462.
 (17) Mullins, C. S.; Grapperhaus, C. A.; Kozlowski, P. M. *J. Biol. Inorg. Chem.* **2006**, *11*, 617-625.
 (18) Shearer, J.; Long, L. M. *Inorg. Chem.* **2006**, *45*, 2358-2360.

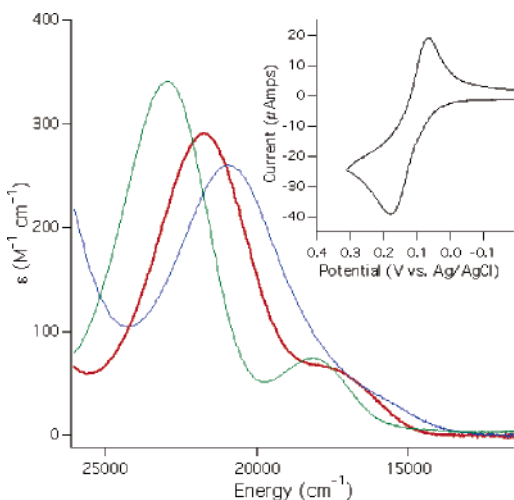


Figure 3. Electronic absorption spectra for $[\text{Me}_4\text{N}](\text{Ni}^{\text{II}}(\text{BEAM}))$ (red bold line), $[\text{Et}_4\text{N}]_2(\text{Ni}^{\text{II}}(\text{emi}))$ (green line), and $(\text{btmp-dmed})\text{Ni}$ (blue line). The inset depicts the cyclic voltammograms obtained for $[\text{Me}_4\text{N}](\text{Ni}^{\text{II}}(\text{BEAM}))$ (MeCN; 0.1 M Bu_4NPF_6 ; $\nu = 100 \text{ mV s}^{-1}$; room temperature).

these ligand-field transitions to higher energies are consistent with our DFT calculations, which show that the normalized unfilled $\text{Ni}(3d_{x^2-y^2})/\text{S}/\text{N}(\sigma)^*$ orbital progresses to higher energy as more amides are included in the primary coordination sphere.

It is known that bis-amide NiN_2S_2 complexes have more negative $\text{Ni}^{\text{II/III}}$ redox couples than structurally related bis-amine complexes.^{11a} We observe a quasireversible $\text{Ni}^{\text{II/III}}$ redox couple for $[\text{Me}_4\text{N}](\text{Ni}^{\text{II}}(\text{BEAM}))$ at 0.12(1) V vs Ag/AgCl (Figure 3, inset). $[\text{Et}_4\text{N}]_2(\text{Ni}^{\text{II}}(\text{emi}))$ displays a more negative reversible $\text{Ni}^{\text{II/III}}$ couple at -0.34 V vs Ag/AgCl.^{11a} Our DFT calculations suggest that both of these redox couples are mostly Ni-based because the percentage of S character comprising the redox-active HOMOs are fairly low. In contrast, $(\text{btmp-dmed})\text{Ni}$ displays an irreversible oxidation wave at 0.41 V vs Ag/AgCl.⁷ It has been speculated that this oxidation is ligand-based, leading to disulfide formation and complex decomposition.⁷ This is in line with our DFT studies that suggest that the HOMO of $(\text{btmp-dmed})\text{Ni}$ is mostly S-based.

$[\text{Ni}(\text{SOD}^{\text{M1}})]$ displays a $\text{Ni}^{\text{II/III}}$ couple at 0.70 V vs Ag/AgCl.^{18,19} If $[\text{Ni}(\text{SOD}^{\text{M1}})]$ displayed similar systematic changes in electrochemical behavior upon going from an amine/amide to a bis-amine motif, then it would become inactive with respect to SOD catalysis. Not only would it become inactive because of a poor redox potential match with $\text{O}_2^{\bullet-}$, but the oxidation would become mostly S-based, leading to metalloprotein decomposition. These data therefore suggest why nature has chosen the amine/amide over the bis-amine motif in NiSOD. However, these electrochemical data do not suggest why the bis-amide motif is not utilized by NiSOD. If a similar change in the electrochemical behavior is obtained upon bis-amide coordination, then $[\text{Ni}(\text{SOD}^{\text{M1}})]$ would still yield a viable SOD from an electro-

(19) To our knowledge, the NiSOD redox couple has not been reported.

chemical perspective; the $\text{Ni}^{\text{II/III}}$ couple would be mainly Ni in character, and the potential of the couple would match well with $\text{O}_2^{\bullet-}$. This begs the question, why does NiSOD not utilize the bis-amide motif?

Our DFT studies demonstrated that in these $\text{Ni}^{\text{II}}\text{N}_2\text{S}_2$ complexes the $\text{Ni}/\text{S}(\pi)^*$ HOMO increases in energy upon an increase in the amide content within the primary coordination sphere. Grapperhaus and others have linked this “activation” of the $\text{M}-\text{S}(\pi)^*$ orbitals with an increase in the S-based reactivity of metal thiolate complexes.^{6,17,20} $[\text{Et}_4\text{N}]_2(\text{Ni}^{\text{II}}(\text{emi}))$ is highly reactive toward O_2 , resulting in the full conversion to an oxidized species within a matter of minutes in MeCN. In contrast, $(\text{btmp-dmed})\text{Ni}$ is stable toward O_2 in solution. We find that $[\text{Me}_4\text{N}](\text{Ni}^{\text{II}}(\text{BEAM}))$ is also stable in solution toward O_2 for at least a week in MeCN. This implies that the mixed amide/amine motif of NiSOD would afford the active-site-enhanced stability toward oxygenation relative to the bis-amide derivative.

The electrochemical data suggest that $\text{Ni}^{\text{III}}(\text{BEAM})$ should be isolable. Attempts to produce and isolate $\text{Ni}^{\text{III}}(\text{BEAM})$ via the one-electron oxidation of $[\text{Me}_4\text{N}](\text{Ni}^{\text{II}}(\text{BEAM}))$ have thus far been unsuccessful. Even at low temperatures (dry ice/acetone bath), the oxidation of propionitrile solutions of $[\text{Ni}^{\text{II}}(\text{BEAM})](\text{Me}_4\text{N})$ produces a short-lived purple/blue species that quickly decomposes to a white insoluble solid. We are currently attempting to trap this purple/blue species for further analysis.

We note that $(\text{Ni}^{\text{II}}(\text{BEAM}))^-$ does not display SOD activity using the xanthine/xanthine oxidase assay of Tabbi et al.²¹ This lack of activity may be due to either the instability of the Ni^{III} adduct, the oxidation of the thiolate S atoms via $\text{H}_2\text{O}_2/\text{O}_2^{\bullet-}$, or the lack of a suitable axial ligand to Ni that may be important for catalysis.²²

In summary, this study suggests why NiSOD utilizes an amide and amine ligand to Ni. It appears that the combination of these ligands in an $\text{Ni}^{\text{II}}\text{N}_2\text{S}_2$ coordination environment (1) ensures a Ni-centered one-electron-oxidation process, (2) appropriately tunes the $\text{Ni}^{\text{II/III}}$ redox potential for SOD catalysis, and (3) provides the thiolate S atoms protection from oxygenation by O_2 , as has been previously suggested.^{16–18}

Acknowledgment. The University of Nevada, Reno (UNR), is acknowledged for financial support. We thank Prof. V. J. Catalano (UNR) for performing the X-ray crystallographic analysis.

Supporting Information Available: Experimental details, crystal structure tables, coordinates, energy level diagrams, isosurface plots from the DFT calculations, and the CIF file for $[\text{Me}_4\text{N}](\text{Ni}^{\text{II}}(\text{BEAM}))\cdot\text{MeCN}\cdot\text{H}_2\text{O}$. This material is available free of charge via the Internet at <http://pubs.acs.org>.

IC061604S

- (20) Ashby, M. T.; Enemark, J. H.; Lichtenberger, D. L. *Inorg. Chem.* **1998**, *27*, 191–197.
 (21) Tabbi, G.; Driessen, W. L.; Reedijk, J.; Bonomo, R. P.; Veldman, N.; Spek, A. L. *Inorg. Chem.* **1997**, *36*, 1168–1175.
 (22) Bryngelson, P. A.; Arobo, S. E.; Pinkham, J. L.; Cabelli, D. E.; Maroney, M. J. *J. Am. Chem. Soc.* **2004**, *126*, 460–461.